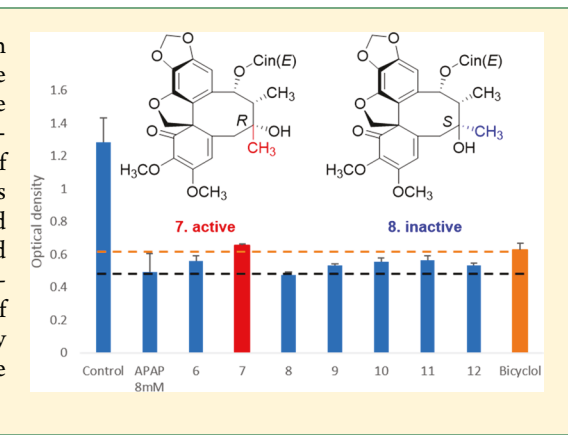


Hepatoprotective Tetrahydrobenzocyclooctabenzofuranone Lignans from *Kadsura longipedunculata*

Jiabao Liu,^{†,∥} Pankaj Pandey,^{‡,∥} Xiaojuan Wang,[⊥] Kamesha Adams,[‡] Xinzhu Qi,[†] Jiabao Chen,[†] Hua Sun,[†] Qi Hou,[†] Daneel Ferreira,[§] Robert J. Doerksen,[‡] Mark T. Hamann,^{*,⊥} and Shuai Li*,[†]

Supporting Information

ABSTRACT: Three new tetrahydrobenzocyclooctabenzofuranone lignan glucosides, longipedunculatins A–C (1–3), a new dibenzocyclooctadiene lignan glucoside, longipedunculatin D (4), a new dibenzocyclooctadiene lignan (5), five new tetrahydrobenzocyclooctabenzofuranone lignans (6–10), and two new simple lignans (11, 12) were isolated from the roots of *Kadsura longipedunculata*. Their structures and absolute configurations were established using a combination of MS, NMR, and experimental and calculated electronic circular dichroism data. Compound 7 showed moderate hepatoprotective activity against *N*-acetyl-*p*-aminophenolinduced toxicity in HepG2 cells with a cell survival rate at 10 μ M of 50.8%. Compounds 2, 7, and 12 showed significant in vitro inhibitory effects with an inhibition rate of 55.1%, 74.9%, and 89.8% on nitric oxide production assays at 10 μ M.



onalcoholic fatty liver disease (NAFLD) is the most common cause of liver disease worldwide, and rates have been increasing in parallel with those of obesity and diabetes. 1,2 It is a global health concern, as 25-30% of the NAFLD cases progress to severe chronic liver diseases such as nonalcoholic steatohepatitis (NASH),³ which includes serious inflammation and hepatocyte damage. Data suggested that hepatic steatosis with inflammation substantially increases the progression toward NASH.4 Due to the burden of the disease, and without an efficient drug approved by the U.S. Food and Drug Administration, it is important to identify new chemical entities for the treatment of NAFLD. There is growing evidence that N-acetyl-p-aminophenol (APAP, acetaminophen/paracetamol) induces liver injury including chronic liver disease and NAFLD.5 Thus, compounds having a hepatoprotective effect against APAP-induced toxicity may have a potential therapeutic effect on NAFLD. Our published data suggested that tetrahydrobenzocyclooctabenzofuranone lignans from Kadsura longipedunculata Finet et Gagnep. (Magnoliaceae) possess hepatoprotective effects against APAP-induced toxicity in HepG2 cells.^{6,7} A large number of phytochemical and pharmaceutical studies on the genus Kadsura have showed that it is a principal source of dibenzocyclooctadiene lignans that exhibit various beneficial bioactivities such as hepatoprotective, 8-11 antioxidant, 12,13 antiviral, 14,15 and neuroprotective effects. 16 Thus far, 63

spirobenzofuranoid dibenzocyclooctadienes are among the 300 lignans that were isolated and identified from plants of the *Kadsura* genus. Our interest in searching for new dibenzocyclooctadiene lignans with hepatoprotective activities led to the isolation of 12 new lignans from the roots of *K. longipedunculata*, including three new tetrahydrobenzocyclooctabenzofuranone lignan glucosides (1-3) and a new dibenzocyclooctadiene lignan (5), five new tetrahydrobenzocyclooctadiene lignan (5), five new tetrahydrobenzocyclooctabenzofuranone lignans (6-10), and two new simple lignans (11, 12). Their structures and absolute configurations were established through a combination of physicochemical and electronic circular dichroism data analysis. In addition, the isolated compounds were assayed for their in vitro anti-inflammatory and hepatoprotective activities.

■ RESULTS AND DISCUSSION

A 95% ethanol extract of the dried roots of K. longipedunculata was subjected to a combination of chromatographic steps on silica gel, Sephadex LH-20, and semipreparative HPLC to afford the new longipedunculatins A–D (1–4), the new longipedlignans K–R (5–12), and the known lignan

Received: June 24, 2019 Published: September 26, 2019



[†]State Key Laboratory of Bioactive Substance and Function of Natural Medicines, Institute of Materia Medica, Chinese Academy of Medical Sciences & Peking Union Medical College, Beijing 100050, People's Republic of China

^LDepartment of Drug Discovery and Biomedical Sciences, College of Pharmacy, Medical University of South Carolina, Charleston, South Carolina 29425, United States

[‡]Department of BioMolecular Sciences, Division of Medicinal Chemistry, and [§]Division of Pharmacognosy, Research Institute of Pharmaceutical Sciences, School of Pharmacy, University of Mississippi, University, Mississippi 38677-1848, United States

$$Ang = 3" \underbrace{\begin{array}{c} 4"CH_3 \text{ O} \\ 2" \text{ of } 5" \text{ CH}_3 \text{ O} \\ 2" \text{ of } 5" \text{ CH}_3 \text{ O} \\ 3" \underbrace{\begin{array}{c} 5" \text{ CH}_3 \text{ O} \\ 2" \text{ of } 5" \text{ CH}_3 \text{ O} \\ 4" \text{ CH}_3 \text{ O} \\ 6" \text{ O} \\$$

Figure 1. Structures of compounds 1-15.

Table 1. 1 H NMR Data of 1–4 in Methanol- d_{4} (δ in ppm, J in Hz, 500 MHz)

position	1	2	3	4
6	6.74, s	6.33, s	6.65, s	6.37, s
7	5.71, d (7.0)	5.60, d (6.5)	5.94, d (7.0)	4.63, br s
8	2.05, m	1.98, m	1.97, m	1.84, m
9	1.06, d (7.0)	1.02, d (7.0)	0.90, d (7.0)	1.13, d (7.0)
6'	6.30, s	6.27, d (2.0)	6.34, d (2.0)	6.60, s
$7'\alpha$	2.38, dd (12.5, 16.0)	2.33, dd (12.0, 16.0)	2.31, dd (12.0, 15.5)	2.60, dd (7.0, 13.0)
$7'\beta$	2.70, dd (4.5, 16.0)	2.65, ddd (2.0, 6.0, 16.0)	2.66, ddd (2.0, 6.0, 15.5)	2.48, br d (13.0)
8'	1.80, m	1.76, m	1.73, m	2.00, m
9'	0.93, d (7.0)	0.87, d (7.0)	0.84, d (7.0)	0.89, d (7.0)
11α	4.50, d (9.0)	4.43, d (9.0)	4.52, d (9.0)	5.92, d (2.0)
11β	4.37, d (9.0)	4.32, d (9.0)	4.36, d (9.0)	
OCH ₃ -3				3.76, s
OCH ₃ -4'	3.64, s	3.58, s	3.65, s	3.83, s
OCH ₃ -5'	4.07, s	4.02, s	4.04, s	
2"			2.07, m	
$3''\alpha$	5.78, br q (7.0)	5.74, br q (7.0)	1.54, dq (7.0, 7.0)	
$3''\beta$			1.33, dq (7.0, 7.0)	
4"	1.71, d (7.0)	1.67, d (7.0)	0.81, d (7.0)	
5"	1.75, s	1.69, s	0.87, t (7.0)	
1‴	4.90, d (7.0)	4.91, d (7.5)	4.79, d (7.5)	4.97, d (7.5)
2‴	3.54, m	3.44, dd (7.5, 8.5)	3.47, m	3.48, m
3‴	3.52, m	3.42, dd (8.5, 8.5)	3.46, overlapped	3.40, overlapped
4‴	3.43, dd (9.0,8.5)	3.43, dd (8.5, 8.5)	3.35, overlapped	3.45, overlapped
5‴	3.51, m	3.29, overlapped	3.43, overlapped	3.45, overlapped
6‴a	3.96, br d (12.0)	3.79, dd (12.0, 2.0)	3.90, dd (12.0, 2.0)	3.82, dd (12.0, 2.0)
6‴b	3.75, dd (12.0, 6.0)	3.72, dd (12.0, 4.5)	3.68, dd (12.0, 6.0)	3.72, dd (12.0, 5.0)

heteroclitin J (13)¹⁷ (Figure 1). The structure of 13 was determined by spectroscopic/spectrometric data analysis and comparison to literature values.

Longipedunculatin A (1) was assigned a molecular formula of $C_{32}H_{40}O_{13}$ based on its HRESIMS (m/z 655.2367 [M + Na]⁺, calcd for 655.2361) and ¹³C NMR data. The ¹³C NMR and HSQC spectra of 1 showed 32 resonances, including 18 carbons for an α,β -unsaturated carbonyl group (δ_C 197.5), a pentasubstituted aromatic moiety, four olefinic carbons at δ_{C} 133.8, 159.8, 121.2, and 150.2, three methines at $\delta_{\rm C}$ 33.0, 44.1, and 80.2, a methylene at $\delta_{\rm C}$ 41.0, a quaternary carbon at $\delta_{\rm C}$ 66.4, and two secondary methyls at $\delta_{\rm C}$ 21.9 and 10.1 for a ${\rm C}_{18}$ framework. The ¹H NMR data (Table 1) displayed two aromatic singlets at $\delta_{\rm H}$ 6.74 (H-6) and 6.30 (H-6'), an olefinic proton at $\delta_{\rm H}$ 5.78 (H-3"), two O-methyl singlets at $\delta_{\rm H}$ 4.07 (3H) and 3.64 (3H), two secondary methyl doublets at $\delta_{\rm H}$ 1.06 (CH₃-9) and 0.93 (CH₃-9'), an oxygenated methine at $\delta_{\rm H}$ 5.71 (H-7), a methylene at $\delta_{\rm H}$ 2.70 (H-7' β) and 2.38 (H-7' α), two methines at $\delta_{\rm H}$ 2.05 (H-8) and 1.80 (H-8'), and an oxygenated methylene group at $\delta_{\rm H}$ 4.50 (1H, d, J=9.0 Hz) and 4.37 (1H, d, J=9.0 Hz). The 1 H $^{-1}$ H COSY correlations from H-8 ($\delta_{\rm H}$ 2.05) and H-7 ($\delta_{\rm H}$ 5.71) to Me-9 ($\delta_{\rm H}$ 1.80) and the HMBC cross-peaks of H-7 ($\delta_{\rm H}$ 5.71), H-7' α ($\delta_{\rm H}$ 2.38), and H-7' β ($\delta_{\rm H}$ 2.70) with C-6 ($\delta_{\rm C}$ 110.2) and C-6' ($\delta_{\rm C}$, 121.2), respectively, indicated the presence of a cyclooctene moiety (Figure 2). The presence of two characteristic doublets at $\delta_{\rm H}$

Figure 2. Structure and key HMBC ($H\rightarrow C$) correlations and ROESY (\leftrightarrow) correlations of 1.

4.50 and 4.37 (each d, J = 9.0 Hz) in the ¹H NMR spectrum, combined with the presence of a quaternary carbon in the ¹³C NMR spectrum ($\delta_{\rm C}$ 66.4) suggested that 1 is a modified dibenzocyclooctadiene-type lignan possessing a spirobenzofuranoid moiety.6 Additionally, the 13C NMR data (Table 2) displayed an α,β -unsaturated carbonyl group ($\delta_{\rm C}$ 169.9), two olefinic carbons ($\delta_{\rm C}$ 136.4 and 129.4), and two allylic methyls ($\delta_{\rm C}$ 21.0 and 15.9). Combined with the HMBC crosspeaks of Me-5" [$\delta_{\rm H}$ 1.75 (3H, br s)] and Me-4" [$\delta_{\rm H}$ 1.71 (3H, d)] with C-1" ($\delta_{\rm C}$ 169.9) and C-2" ($\delta_{\rm C}$ 129.4), these data indicated the presence of an angeloyloxy group. In addition, the ¹³C NMR spectrum revealed the characteristic signals for a glucose moiety (δ_C 104.3, 75.0, 77.6, 71.5, 78.3, and 62.6). The large coupling constant (7.0 Hz) of the anomeric proton implied the β -configuration. The acid hydrolysis of 1 liberated D-glucopyranose, which was identified with HPLC analysis by comparing with authentic sugar samples after derivatization (Figure S1, Supporting Information). 18 The HMBC crosspeaks of glucose H-1 ($\delta_{\rm H}$ 4.90) with C-5 ($\delta_{\rm C}$ 148.3) and of H-7 $(\delta_{\rm H} 5.71)$ with C-1" $(\delta_{\rm C} 169.9)$ revealed that the glucosyl and angeloyloxy moiety were located at C-5 and C-7, respectively.

The relative configuration of 1 was assigned based on the NOESY correlations between H-6/H-7/H-8, suggesting β -

orientations of H-7 and H-8 and an α -orientation of CH₃-9. The α -orientation of CH₃-9' was supported by the NOESY correlation between CH₃-9/CH₃-9'. The NOESY correlation between H-6/H-1''' supported the location of the glucose moiety at C-5.

The experimental electronic circular dichroism (ECD) spectrum of compound 1 exhibited negative Cotton effects at 222 and 319 nm and a positive Cotton effect at 370 nm. The experimental and calculated ECD spectra of 1 matched well (Figure 3). The calculated ECD spectrum exhibited strong

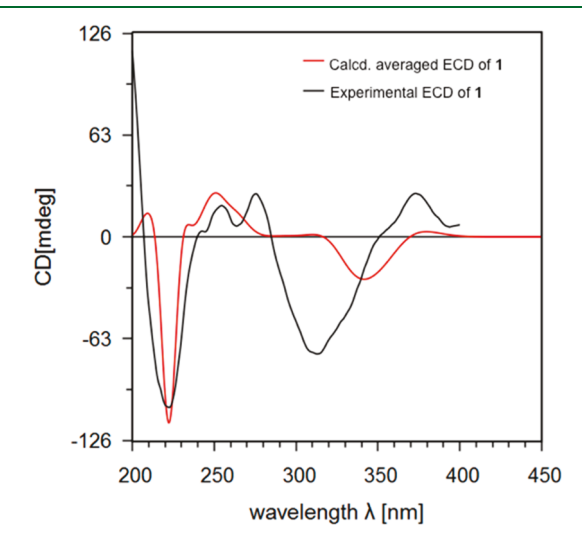


Figure 3. Experimental and calculated averaged Boltzmann-weighted ECD spectra of 1 (red) in MeOH. The σ -value (artificial line broadening) was set to 0.17 eV.

negative Cotton effects (CEs) at \sim 220 and \sim 340 nm [slight deviation (\sim 20 nm) from experimental wavelength] and a weak positive CE at \sim 380 nm. On the basis of the above data and extensive 2D NMR experiments, the cyclooctene moiety in 1 was determined to be in a twisted boat conformation possessing a (7R, 8R, 2'S, 8'R) absolute configuration. Thus, the structure of longipedunculatin A (1) was defined as shown in Figure 2.

Longipedunculatin B (2) was obtained as a light yellow, amorphous powder. The HRESIMS ion at m/z 633.2550 [M + H]⁺ and ¹³C NMR data of 2 established its molecular formula as $C_{32}H_{40}O_{13}$, an isomer of 1. The UV, IR, NMR, and ECD data showed that 2 was a (7R,8R,2'S,8'R)-tetrahydrobenzocyclooctabenzofuranone-type lignan. The NMR data of 2 were similar to those of 1, except for the changes involving the location of the glucose moiety. The HMBC cross-peak of glucose H-1" $(\delta_{\rm H}$ 4.91) with C-4 $(\delta_{\rm C}$ 130.4) indicated that the glucose moiety is located at C-4. Acid hydrolysis and the large coupling constant (7.5 Hz) of the anomeric proton of 2 suggested the presence of a β -D-glucosyl moiety. Thus, the structure of longipedunculatin B (2) was defined as shown in Figure 1.

Longipedunculatin C (3) was isolated as a light yellow, amorphous powder. The molecular formula was established as $C_{32}H_{42}O_{13}$ by HRESIMS at m/z 657.2531 [M + Na]⁺ and ¹³C NMR data. The NMR data of 3 exhibited a close resemblance with 1, except for two more hydrogens than 1. The ¹³C NMR data and the HMBC cross-peaks of C-1" ($\delta_{\rm C}$ 178.1) with H-7 ($\delta_{\rm H}$ 5.94), H-3" ($\delta_{\rm H}$ 1.54), and H-5" ($\delta_{\rm H}$ 0.87) showed that a 2-methylbutyryl group is connected to C-7. The ECD and

NOESY data suggested the same (7*R*, 8*R*, 2'*S*, 8'*R*) absolute configuration of this new tetrahydrobenzocyclooctabenzo-furanone lignan. Thus, the structure of longipedunculatin C (3) was defined as shown in Figure 1.

Figure 4. Structure and key HMBC ($H\rightarrow C$) correlations and ROESY (\leftrightarrow) correlations of 4.

Longipedunculatin D (4) was assigned a molecular formula of $C_{27}H_{34}O_{12}$, according to its HRESIMS (m/z 573.1958 [M + Na]+) and ¹³C NMR data. The NMR spectra exhibited the signals of a decasubstituted biphenyl moiety ($\delta_{\rm H}$ 6.60, s, and 6.37, s; $\delta_{\rm C}$ 140.3, 121.1, 142.7, 137.2, 150.1, 103.5 and 135.3, 120.0, 149.1, 136.3, 150.2, 111.7). The ¹H NMR data indicated two secondary methyl doublets at $\delta_{\rm H}$ 1.13 (H₃-9) and 0.89 (H₃-9'), a methine proton at $\delta_{\rm H}$ 1.84 (H-8), an oxymethine at $\delta_{\rm H}$ 4.63 (H-7), and a methylene at $\delta_{\rm H}$ 2.60 (H- $7'\alpha$) and 2.48 (H-7' β). Combined with the HMBC crosspeaks of H-7 with C-8 and C-8', H₃-9 and H-6 with C-7, and H-6' with C-1', C-2', and C-7', these data suggested the presence of a cyclooctadiene moiety (Figure 4). The CH₃O-3 and CH₃O-4' locations were determined by the HMBC crosspeaks of CH₃O-3 ($\delta_{\rm H}$ 3.76, s) with C-3 ($\delta_{\rm C}$ 142.7) and of CH₃O-4' ($\delta_{\rm H}$ 3.83, s) with C-4' ($\delta_{\rm C}$ 136.3). The HMBC crosspeak of glucose H-1 ($\delta_{\rm H}$ 4.97) with C-5' ($\delta_{\rm C}$ 150.2) showed the glucosylation position to be at C-5'. The experimental ECD curve of 4 displayed sequential negative and positive Cotton effects near 254 and 210 nm, respectively, indicating a (P)-biphenyl absolute configuration. The calculated ECD spectrum of 4 also exhibited strong sequential negative (~254 nm) and positive (~210 nm) CEs and matched closely with the experimental spectrum (Figure 5). The absolute configurations of the remaining stereogenic centers of 4 were defined through NOESY correlations of H-6/H-7 and H-8 and H-6'/CH₃-9', which were in agreement with a cyclooctadiene lignan possessing a twisted boat/chair conformation with a (7R, 8R, 8'R) absolute configuration. Thus, the structure of longipedunculatin D (4) and its (aP, 7R, 8R, 8'R) absolute configuration were established as shown in Figure 1.

Longipedlignan K (5) was obtained as a white, amorphous powder. The HRESIMS data of 5 indicated a positive prominent ion peak at m/z 531.1996 [M + Na]⁺ (calcd for 531.1989), consistent with the molecular formula $C_{29}H_{32}O_8Na$. The UV, IR, and NMR data of 5, similar to those of 4, suggested the presence of a dibenzocyclooctadiene core structure. However, the absence of NMR signals of a glucosyl unit indicated that 5 is a lignan aglycone. The HMBC cross-peaks of the four methoxy groups with C-4′, C-3′ and C-3, C-4 showed that the methoxy groups are located at C-4′, C-3′, and C-3, C-4. The presence of signals at δ_H 8.05 (2H, dd, J = 8.0, 1.5 Hz), 7.54 (1H, t, J = 8.0 Hz), and 7.43 (2H, t, J = 8.0

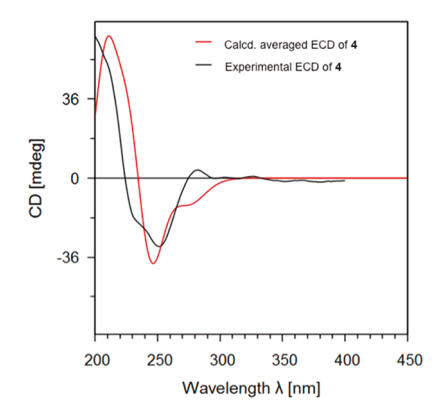


Figure 5. Experimental and calculated averaged Boltzmann-weighted ECD spectra of **4** (red) in MeOH. The σ -value (artificial line broadening) was set to 0.17 eV.

Hz), combined with the ester carbonyl group ($\delta_{\rm C}$ 165.1), indicated a benzoyloxy group in **5**. The HMBC cross-peaks of H-7 ($\delta_{\rm H}$ 5.78) with C-1" ($\delta_{\rm C}$ 165.1) positioned the benzoyloxy group at C-7. ROESY correlations of H-6/H-7/H-8, H-6'/H-7' α , and H₃-9/H₃-9' showed that the benzoyloxy group, CH₃-9, and CH₃-9' were cofacial and likely α -oriented (Figure 6).

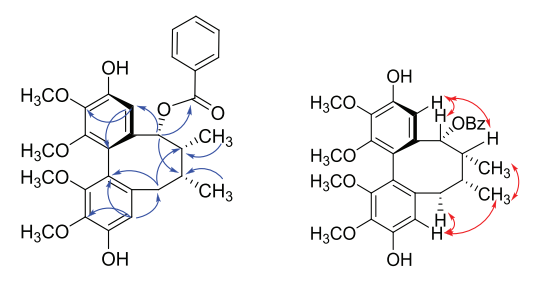


Figure 6. Structure and key HMBC ($H\rightarrow C$) correlations and ROESY (\leftrightarrow) correlations of **5**.

The experimental ECD curve of 5 exhibited sequential positive and negative Cotton effects at 249 and 210 nm, respectively, suggesting that 5 possesses an *M*-biphenyl configuration. The calculated ECD spectrum of 5 exhibited identical positive and negative Cotton effects at ca. 250 and 210 nm as observed in the experimental spectrum. Figure 7 depicts overlays of the experimental and the calculated averaged Boltzmann-weighted ECD spectra of 5 (red) in MeOH at the B3LYP/6-311+G(2d,p) level. Thus, the structure of 5 was in agreement with a cyclooctadiene lignan with a twisted boat conformation having an (aM, 7'R, 8'R, 7R) absolute configuration. Based on

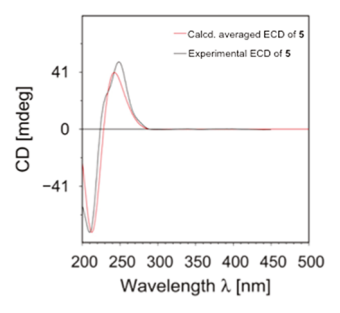


Figure 7. Experimental and calculated averaged Boltzmann-weighted ECD spectra of 5 (red) in MeOH. The σ -value (artificial line broadening) was set to 0.21 eV.

these data, longipedlignan K (5) was defined as shown in Figure 6.

Longipedlignan L (6) had a molecular formula of C₂₃H₂₂O₈ as determined by the HRESIMS $(m/z 449.1210 [M + Na]^{+})$ and ¹³C NMR data. The NMR data, especially the singlets at $\delta_{\rm H}$ 6.70 and 6.43 together with two characteristic methylene proton doublets at $\delta_{\rm H}$ 4.92 and 4.43 in the ¹H NMR spectrum, and a quaternary carbon at $\delta_{\rm C}$ 67.1 in the ¹³C NMR spectrum suggested that 6 is a tetrahydrobenzocyclooctabenzofuranonetype lignan. However, the two carbonyl carbon signals at $\delta_{\rm C}$ 190.9 and 176.5 of 6 were unusual compared to the C₁₉ tetrahydrobenzocyclooctabenzofuranone-type compounds discussed above and instead were structurally characteristic signals of interiotherin D. 21 An ester carbonyl carbon at $\delta_{\rm C}$ 169.6 and a relatively deshielded methyl group at $\delta_{\rm H}$ 1.67 indicated the presence of an acetyl group. The HMBC crosspeak between H-7 ($\delta_{\rm H}$ 5.98) and C-1" ($\delta_{\rm C}$ 169.6) revealed that the acetyl group is located at C-7. The ROESY correlations of H-6'/H-7' and H-6/H-7/H-8 suggested the α -orientations of the acetyl group, CH₃-9, and CH₃-9' (Figure 8). The

Figure 8. Structure and key HMBC ($H\rightarrow C$) correlations and ROESY (\leftrightarrow) correlations of **6**.

experimental ECD spectrum of 6 displayed negative Cotton effects at 308 and 214 nm and positive Cotton effects at 386 and 258 nm. The calculated averaged ECD spectrum of 6 in MeOH was in accordance with the experimental spectrum (Figure 9). Thus, the (7R, 8R, 2'S, 8'R) absolute configuration and structure of longipedlignan L¹ (6) was established as shown in Figure 8.

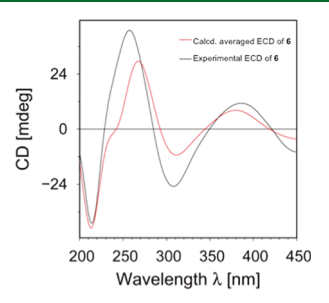


Figure 9. Experimental ECD and calculated averaged Boltzmann-weighted ECD spectra of 6 (red) in MeOH. The σ -value (artificial line broadening) was set to 0.21 eV.

Longipedlignans M (7) and N (8) had the same molecular formula of $C_{31}H_{32}O_9$ by HRESIMS (m/z 569.1792 [M + Na]⁺ and 569.1785 [M + Na]⁺, respectively). The ¹³C NMR and HSQC spectra of compounds 7 and 8 exhibited 19 carbon atoms, including an α , β -unsaturated carbonyl group (δ_C 195.2 and 195.6, respectively), a pentasubstituted aromatic ring, four olefinic carbons (δ_C 131.8, 156.6, 121.6, 145.5 and δ_C 131.7, 156.8, 121.8, 145.7, respectively), a quaternary carbon (δ_C 66.3 and δ_C 67.1, respectively), three methines (δ_C 72.6, 48.0, 81.0

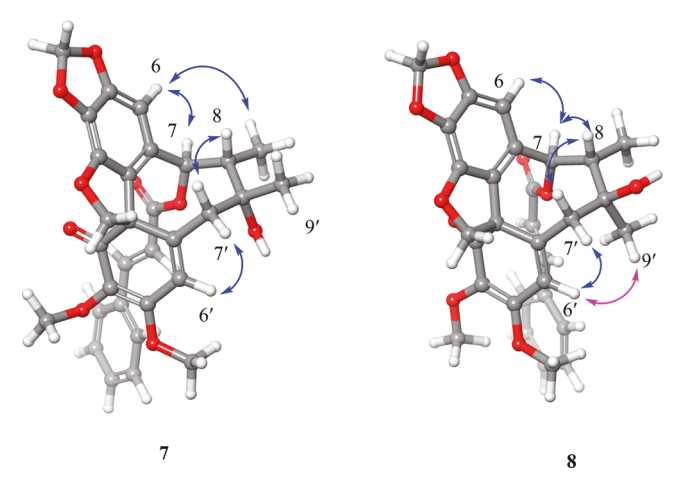


Figure 10. Comparison of key ROESY (blue \leftrightarrow) correlations of 7 and 8 and characteristic ROESY correlation (magenta \leftrightarrow) of 8.

and $\delta_{\rm C}$ 75.7, 50.7, 78.4, respectively), two methylenes ($\delta_{\rm C}$ 79.2, 44.6 and $\delta_{\rm C}$ 79.5, 46.9, respectively), and two secondary methyls ($\delta_{\rm C}$ 31.3, 17.6 and $\delta_{\rm C}$ 24.1, 17.8, respectively), suggesting that both 7 and 8 are tetrahydrobenzocyclo-octabenzofuranone-type lignans. The 1D and 2D NMR spectra also showed an (*E*)-cinnamoyl group in 7 and 8 (Tables 3 and 4). The NMR data of 7 and 8 were similar to those of longipedlignans F (14) and G (15), except for changes involving the C-7 substituents. The C-7 benzoyl groups in 14 and 15 were replaced by (*E*)-cinnamoyl groups in 7 and 8. The ECD and ROESY data for 7 and 8 (Figure 10) suggested a (7*R*, 8*S*, 2'*S*, 8'*S*) absolute configuration for 7 and a (7*R*, 8*S*, 2'*S*, 8'*S*) absolute configuration for 8. Thus, the structures of longipedlignans M (7) and N (8) were formulated as shown in Figure 1.

Longipedlignans O (9) and P (10) had molecular formulas of C₂₉H₂₈O₁₀ and C₂₄H₂₆O₁₀, respectively, as derived from the HRESIMS ions at m/z 559.1581 [M + Na]⁺ (calcd 559.1575) and 497.1436 [M + Na]⁺ (calcd 497.1418), respectively. The UV, IR, and NMR spectra established that 9 and 10 both possessed a tetrahydrobenzocyclooctabenzofuranone-type lignan skeleton, similar to heteroclitin J (13).¹⁷ An angeloyl group in 13 was changed to a benzoyl group in 9 and to an acetyl group in 10. Since the ECD curves of 9 and 10 were quite similar to that of 13, which had positive Cotton effects near 360 and 270 nm and negative Cotton effects near 240 and 210 nm, a (2'S) configuration is indicated. The ROESY correlations of H-7'/H-8'/H-6' showed that the oxetane ring system should be α -oriented; correlations of H-6/H-7/H-8 and H_3-9'/H_3-9 indicated the α -orientations of CH_3-9' and CH₃-9 in 9 and 10 (Figure 11). Since ROESY correlations of HO-1' with other protons were not observed, its orientation could not be elucidated. Therefore, the configurations of 9 and 10 could be assigned tentatively as $(1'S^*, 2'S, 6'S, 7'S, 8'S, 7R,$ 8R), as shown in Figure 1.

The molecular formula of longipedlignan Q (11) was calculated as $C_{22}H_{30}O_7$ from the HRESIMS ion at m/z 429.1893 [M + Na]⁺. The molecular formula was in agreement with eight indices of hydrogen deficiency associated with two benzene moieties. Analysis of the ¹³C NMR data indicated 12 aromatic carbons, three methine carbons, a methylene group, and two secondary methyls, indicating a lignan with a biphenyldimethylbutane skeleton. The two pairs of m-coupled aromatic protons [δ_H 6.54 (1H, d, J = 2.0 Hz, H-6) and 6.51

Table 2. 13 C NMR Data of 1–4 in Methanol- d_4 (δ in ppm, 125 MHz)

position	1	2	3	4
1	127.5	119.9	126.9	140.3
2	123.2	133.2	123.8	121.1
3	151.7	152.3	151.9	142.7
4	132.9	130.4	133.3	137.2
5	148.3	155.4	148.2	150.1
6	110.2	109.1	110.6	103.5
7	80.2	80.0	78.5	84.6
8	44.1	44.0	44.1	44.4
9	10.1	10.1	9.6	20.5
1'	150.2	150.4	151.4	135.3
2'	66.4	65.9	66.7	120.0
3'	197.5	197.8	198.3	149.1
4'	133.8	133.8	133.7	136.3
5'	159.8	160.0	160.6	150.2
6'	121.2	121.4	120.8	111.7
7′	41.0	41.0	41.1	39.6
8'	33.0	33.1	33.2	36.8
9'	21.9	21.9	21.8	15.5
11	79.0	79.3	78.9	102.5
OCH ₃ -3				60.0
OCH ₃ -4'	59.7	59.7	59.8	61.7
OCH ₃ -5'	58.9	58.9	58.9	
1"	169.9	169.8	178.1	
2"	129.4	129.3	41.7	
3"	136.4	136.8	28.1	
4"	15.9	15.9	11.9	
5"	21.0	21.0	16.3	
1‴	104.3	105.7	104.5	102.3
2‴	75.0	75.2	75.0	75.0
3‴	77.6	77.6	77.6	77.9
4‴	71.5	70.8	71.5	71.2
5‴	78.3	78.3	78.3	78.1
6‴	62.6	62.0	62.5	62.3

(1H, d, J = 2.0 Hz, H-2), $\delta_{\rm H}$ 6.39 (1H, d, J = 2.0 Hz, H-2') and 6.38 (1H, d, J = 2.0 Hz, H-6')] and four singlets for methoxy groups at $\delta_{\rm H}$ 3.86 (3H), 3.83 (3H), 3.79 (3H), and 3.78 (3H) suggested that the methoxy groups are located at C-3, C-4 and C-3', C-4'. The calculated ECD spectrum of 11 (7S, 8R, 8'R) showed a negative Cotton effect at ~216 nm that matched the experimental ECD spectrum (Figure 12). The negative Cotton effect of 11 at around 216 nm suggested the (7S) absolute configuration. Combined with the NOE correlations of H-7/H-2/H-6 and of H-8'/H-8 and the large coupling constant of H-7 and H-8 ($J_{7,8}$ = 9.5 Hz) and a small coupling constant of H-8 and H-8' (J = 3.0 Hz), these data helped assign the (8R, 8'R) absolute configuration. Thus, the structure of longipedlignan Q (11) and its (7S, 8R, 8'R) absolute configuration were established as shown in Figure 1.

Longipedlignan R (12) was obtained as a pale yellow gum and was assigned a molecular formula of $C_{21}H_{26}O_6$, as deduced from the HRESIMS (m/z 397.1635 [M + Na]⁺) and ¹³C NMR data. In the ¹H NMR spectrum of 12, three methoxy groups [$\delta_{\rm H}$ 3.90 (3H), 3.87 (3H), and 3.86 (3H)], an ABX aromatic spin system [$\delta_{\rm H}$ 6.96 (1H, d, J = 8.0 Hz, H-5), 6.92 (1H, d, J = 1.5 Hz, H-2), and 6.89 (1H, dd, J = 8.0, 1.5 Hz, H-6)], m-coupled aromatic protons [$\delta_{\rm H}$ 6.57 (1H, d, J = 1.5 Hz, H-2') and 6.51 (1H, d, J = 1.5 Hz, H-6')], and two olefinic proton signals [$\delta_{\rm H}$ 6.35 (1H, br dd, J = 15.5, 1.5 Hz, H-7) and 6.16

(1H, dq, J = 15.5, 8.5 Hz, H-8)] of an (E)-double bond were observed. Furthermore, the HMBC cross-peaks of H-7 ($\delta_{\rm H}$ 6.35) with C-1 ($\delta_{\rm C}$ 133.8), C-2 ($\delta_{\rm C}$ 109.3), and C-6 ($\delta_{\rm C}$ 119.0), of H-8 ($\delta_{\rm H}$ 6.16) with C-1 ($\delta_{\rm C}$ 133.8), C-7 ($\delta_{\rm C}$ 130.5), and C-9 ($\delta_{\rm C}$ 18.4), and of H-9 ($\delta_{\rm H}$ 1.88) with C-7 ($\delta_{\rm C}$ 130.5) and C-8 ($\delta_{\rm C}$ 125.0) indicated the presence of a 3,4disubstituted propenylphenyl moiety. The HMBC crosspeaks of H-7 $^{'}$ ($\delta_{\rm H}$ 4.79) with C-1 $^{'}$ ($\delta_{\rm C}$ 136.1), C-2 $^{'}$ ($\delta_{\rm C}$ 102.0), C-6' ($\delta_{\rm C}$ 105.8), C-8' ($\delta_{\rm C}$ 82.3), and C-9' ($\delta_{\rm C}$ 13.3), of H-8' ($\delta_{\rm H}$ 4.33) with C-1' ($\delta_{\rm C}$ 136.1), C-7' ($\delta_{\rm C}$ 73.4), and C-9' ($\delta_{\rm C}$ 13.3), and of H-9' ($\delta_{\rm H}$ 1.17) with C-7' ($\delta_{\rm C}$ 73.4) and C-8' ($\delta_{\rm C}$ 82.3) suggested a 3',4',5'-trisubstituted propenylphenyl moiety. These spectroscopic features combined with the HMBC cross-peak of H-8' ($\delta_{\rm H}$ 4.33) and C-4 ($\delta_{\rm C}$ 145.5) indicated that 12 is an 8-O-4'-type neolignan formed by two phenylpropanoid units. A gauche configuration of 12 was indicated by the $J_{7',8'}$ value of 3.0 Hz^{11} and the NOE correlation of H-7'/H-8'. The (7'S, 8'R) absolute configuration was assigned on the basis of the negative Cotton effect at 244 nm in the ECD spectrum. ²³ Consequently, the structure of longipedlignan R (12) was defined as shown in Figure 1.

All the compounds were evaluated for their in vitro hepatoprotective activity against APAP-induced toxicity in HepG2 (human hepatocellular liver carcinoma cell line) cells, using the hepatoprotective drug bicyclol as the positive control (Table S1, Supporting Information). Compound 7 effected a cell survival rate of 50.8% (cf. bicyclol, 49.0%) at 10 μ M when added into resuscitated HepG2 cells incubated with APAP for 48 h. Notably, 7 in having an (8'R) absolute configuration showed a moderately protective effect on HepG2 cells, but 8, with an (8'S) configuration, was inactive (cell survival rate of 37.0%). Such a result is coincident with our previous report that longipedlignan F (14) was effective but its (8'S)-isomer (15)⁵ was ineffective. In addition, the spirobenzofuranoid moiety is essential for the hepatoprotective effect, as dibenzocyclooctadiene lignans having an (8'R) absolute configuration are inactive. In a cell-based anti-inflammatory assay, compounds 2, 7, and 12 showed significant inhibitory effects with in vitro inhibition rates of 55.1%, 74.9%, and 89.8%, respectively, on nitric oxide (NO) production at 10 μ M (Table S2, Supporting Information). The active metabolite of APAP is known to induce hepatocyte necrosis and to increase the production of inflammatory cytokines and chemokines.² Herein we report the (8'R)-tetrahydrobenzocyclooctabenzofuranone-type lignan (7) as an example, which may protect the damaged HepG2 cells via suppression of the inflammatory response. However, a detailed mechanistic study is needed.

■ EXPERIMENTAL SECTION

General Experimental Procedures. Optical rotations were measured on a JASCO P-2000 polarimeter (JASCO Inc., Easton, MD, USA), and UV spectra with a JASCO V-650 spectrophotometer (JASCO Inc.). ECD spectra were recorded on a JASCO J-815 spectrometer (JASCO Inc.), and IR spectra on a Nicolet 5700 spectrometer (Thermo Electron Corporation, Madison, WI, USA) using an FT-IR microscope transmission method. The 1 H and 13 C NMR spectra were recorded on INOVA-500 (Varian, Inc., Palo Alto, CA, USA) and Bruker AV500-III spectrometers (Bruker, Billerica, MA, USA). Chemical shifts are given in δ (ppm) values relative to those of the solvent signal [CHCl $_{3}$ ($\delta_{\rm H}$ 7.26; $\delta_{\rm C}$ 77.2)]. The standard pulse sequences programmed into the instrument were used for each 2D measurement. HRESIMS data were acquired using an Agilent 6520 Accurate-Mass Q-Tof LC/MS mass spectrometer (Agilent Technologies, Waldbronn, Germany). Analytical reversed-phase

Table 3. ¹H NMR Data of 5–10 in CDCl₃ (δ in ppm, J in Hz, 500 MHz)

position	5	6	7	8	9	10
6	6.99, s	6.43, s	6.41, s	6.42, s	6.41, s	6.26, s
7	5.78, s	5.98, d (5.0)	5.85, s	5.84, s	5.92, d (4.5)	6.06, d (5.0
8	2.17, m	1.82, m	1.86, br q (7.0)	2.03, br q (7.5)	1.95, m	1.83, m
9	0.86, d (7.5)	1.00, d (7.0)	1.29, d (7.0)	1.26, d (7.5)	1.15, d (7.0)	1.05, d (7.0
6'	6.64, s	6.70, s	6.35, s	6.21, s	3.92, s	3.93, s
$7'\alpha$	2.20, dd (9.0, 13.0)	5.78, d (8.5)	2.63, br s	2.71, d (12.5)	3.37, d (9.0)	3.12, d (9.0
$7'\beta$	2.04, br d (13.0)			2.60, d (12.5)		
8'	2.09, m	3.00, m			1.95, m	1.83, m
9'	1.03, d (7.5)	0.94, d (7.0)	1.28, s	1.36, s	1.14, d (7.0)	0.96, d (7.0
10α		6.03, br s	6.02, d (2.0)	6.02, br s	6.01, d (1.5)	5.99, br s
10β		6.00, br s	6.00, d (2.0)	5.96, br s	5.98, d (1.5)	5.97, br s
11α		4.92, d (10.0)	4.72, d (8.0)	4.70, d (8.5)	4.84, d (9.0)	4.88, d (9.5
11β		4.43, d (10.0)	4.20, d (8.0)	4.18, d (8.5)	4.64, d (9.0)	4.73, d (9.5
2"		1.67, s	6.08, d (16.0)	6.11, d (16.0)		1.97, s
3"	8.05, dd (8.0, 1.5)		7.57, d (16.0)	7.58, d (16.0)	7.81, dd (8.0, 1.0)	
4"	7.43, t (8.0)				7.39, t (8.0)	
5"	7.54, t (8.0)		7.49, m	7.50, m	7.56, dt (8.0, 1.0)	
6"	7.43, t (8.0)		7.36, m	7.36, m	7.39, t (8.0)	
7"	8.05, dd (8.0, 1.5)				7.81, dd (8.0, 1.0)	
8"					3.68, s	
9"			7.49, m	7.50, m	3.20, s	
OCH ₃ -3	3.61, s		•	•	•	
OCH ₃ -4	3.97, s					
OCH ₃ -3'	3.58, s					
OCH ₃ -4'	3.94, s		3.58, s	3.62, s		3.74, s
OCH ₃ -5'	•	3.83, s	3.99, s	4.03, s	3.92, s	4.11, s

HPLC was performed on a COSMOSIL 5C₁₈-PAQ Waters column (4.6 \times 250 mm, Waters, Nacalai, San Diego, CA, USA) eluted with H₂O–MeOH (flow rate, 1 mL/min; 220 nm UV detection) at room temperature. Preparative RP-HPLC was performed on a COSMOSIL 5C₁₈-PAQ Waters column (250 \times 10 mm, 5 $\mu m)$ at room temperature. Column chromatography was performed with silica gel (40–63 μm ; Silicycle, Quebec City, QC, Canada), C₁₈ 120 Å reversed-phase silica gel (RP-18; 50 μm ; Silicycle), and Sephadex LH-20 (GE Healthcare Bio-Science AB, Uppsala, Sweden). Fractions were monitored by TLC, and spots were visualized by heating silica gel plates sprayed with 10% H₂SO₄ in EtOH.

Plant Material. The roots of Kadsura longipedunculata were collected in Jiujiang County of Jiangxi Province, People's Republic of China, in March 2010, and identified by Ce-Ming Tan, Institute of Biology Resources, Jiangxi Academy of Science. A voucher specimen (ID-S-2428) is deposited in the herbarium of the Institute of Materia Medica, Chinese Academy of Medical Science and Peking Union Medical College, Beijing, China.

Extraction and Isolation. The air-dried roots of K. longipedunculata (34 kg) were extracted with EtOH-H2O (95:5, v/v) at room temperature, and the extract was concentrated in vacuo to yield a puce residue (2.4 kg), which was chromatographed on a silica gel column, eluting with a petroleum ether-acetone gradient system (50:1, 10:1, 5:1, 3:1, 1:1), acetone, and 80% EtOH, successively, to give fractions 1-14. Fractions 12-14, which showed anti-inflammatory activity, were selected for separation. Fraction 14 (338.5 g) was partitioned between H₂O and EtOAc. Fraction 12 (146.8 g) was subjected to silica gel column chromatography (CHCl3-MeOH, 200:1, 100:1, 50:1 and MeOH) to afford subfractions 12.1-12.5. Fraction 12.1 (36 g) was chromatographed on silica gel (n-hexane-EtOAc, 1:9-1:1) to give four subfractions. Fraction 12.1.2 (10.9 g) was subjected to successive RP-18 column chromatography (65% MeOH-H₂O) to afford five subfractions. Fraction 12.1.2.3 was purified by preparative HPLC (60% MeOH-H2O) to give five fractions, 12.1.2.3A-12.1.2.3E. Fraction 12.1.2.3A (80 mg) was separated by semipreparative HPLC (58% MeOH-H2O) to give 11 (2 mg) and 13 (8 mg). Fraction 12.1.2.3B (100 mg) was

chromatographed by semipreparative HPLC (55% MeOH-H2O) to give 5 (6 mg) and 6 (47 mg). Fraction 12.1.3C3 (43 mg) was purified by semipreparative HPLC (53% MeOH-H₂O) to give 12 (7 mg). Fraction 12.1.3D2 (89 mg) was purified by semipreparative HPLC (54% MeOH-H₂O) to give 7 (15 mg) and 8 (3 mg). Fraction 13.2 was separated by successive silica gel column chromatography (CHCl₃-MeOH, 60:1, 50:1, 30:1 and MeOH) to afford five subfractions. Fraction 13.2.1 was repeatedly subjected to Sephadex LH-20 column chromatography (CHCl₃-MeOH, 1:1) to give five subfractions. Fraction 13.2.1.4 was purified by semipreparative HPLC (60% MeOH-H₂O) to afford 9 (6 mg) and 10 (10 mg). The H₂O extract (60 g) was chromatographed on an RP-18 column (MeOH-H₂O, 20%, 40%, 60%, and 80%, successively), to afford five subfractions. Fraction 14-4 (4.2 g) was subjected to a Sephadex LH-20 column (CHCl₃-MeOH, 1:1) to afford five subfractions. Fraction 14-4A was separated on a silica gel column (CHCl₃-MeOH, 4:1-1:4), and the subfraction 14-4A6 (266 mg) was repeatedly purified by semipreparative HPLC (49% and 52% MeOH-H2O, successively) to afford 1 (12 mg), 2 (15 mg), and 3 (8 mg). Finally, fraction 14-4B (930 mg) was separated by successive silica gel column (CHCl₃-MeOH, 4:1-1:4) chromatography and by semipreparative HPLC (45% MeOH-H₂O and 33% CH₃CN-H₂O) to give 4 (7

(7R,8R,2'5,8'R)-Longipedunculata A (1): yellow, amorphous powder; $[\alpha]_{\rm D}^{20}-12$ (c 0.3, MeOH); UV (MeOH) $\lambda_{\rm max}$ (log ε) 216 (2.58), 330 (1.47) nm; ECD (c 0.3, MeOH) [θ] -6.1×10^3 (222 nm), -3.7×10^3 (319 nm), +1.6 × 10³ (370 nm); IR (microscope transmission) $\nu_{\rm max}$ 3364, 2929, 1715, 1649, 1453, 1307, 1077, 970, 537 cm⁻¹; ¹H and ¹³C NMR data, see Tables 1 and 2; HRESIMS (+) m/z 655.2367 [M + Na]⁺ (calcd for C₃₂H₄₀O₁₃Na, 655.2361).

(7R,8R,2'5,8'R)-Longipedunculata B (2): yellow, amorphous powder; $[\alpha]_{\rm D}^{20}$ –11 (c 0.1, MeOH); UV (MeOH) $\lambda_{\rm max}$ (log ε) 215 (2.57), 332 (1.48) nm; ECD (c 0.1, MeOH) [θ] –1.1 × 10⁴ (213 nm), +3.7 × 10³ (240 nm), –8.9 × 10³ (321 nm), +3.4 × 10³ (373 nm); IR (KBr) $\nu_{\rm max}$ 3386, 2928, 1717, 1648, 1453, 1307, 1056, 967, 537 cm⁻¹; ¹H and ¹³C NMR data, see Tables 1 and 2; HRESIMS (+) m/z 633.255 [M + H]⁺ (calcd for C₃₂H₄₁O₁₃, 633.2542).

Journal of Natural Products

Table 4. 13 C NMR Data of 5–10 in CDCl $_3$ (δ in ppm, 125 MHz)

	-	,	_	0	0	10
position	5	6	7	8	9	10
1	133.7	129.3	130.1	130.4	128.7	128.3
2	121.0	119.0	119.2	118.6	119.8	119.8
3	148.2	143.0	144.2	144.5	144.4	144.3
4	138.6	130.1	130.3	131.3	130.6	130.4
5	150.2	150.7	150.6	150.7	150.4	150.1
6	109.1	102.0	101.4	101.4	101.4	101.4
7	76.3	78.6	81.0	78.4	81.2	78.2
8	41.0	44.1	48.0	50.7	43.1	42.6
9	8.8	10.3	17.6	17.8	11.3	9.9
1'	139.8	132.9	145.5	145.7	59.5	59.4
2'	119.7	67.1	66.3	67.1	66.3	66.1
3′	149.5	190.9	195.2	195.6	191.1	191.9
4′	138.0	176.5	131.8	131.7	134.8	135.6
5'	150.5	151.2	156.6	156.8	156.0	157.3
6′	110.3	126.7	121.6	121.8	73.6	72.7
7'	34.7	140.9	44.6	46.9	75.3	75.0
8'	39.1	30.6	72.6	75.7	33.7	33.3
9′	22.1	19.6	31.3	24.1	18.1	17.9
10		102.5	102.1	102.2	102.3	102.1
11		80.1	79.2	79.5	80.5	80.4
OCH ₃ -3	60.7					
OCH ₃ -4	61.1 ^a					
OCH ₃ -3'	60.3					
OCH ₃ -4'	61.2 ^a		59.1	59.5	59.2	59.4
OCH ₃ -5'		55.9	58.7	59.2	59.8	60.5
1"	165.1	169.6	165.1	165.8	166.6	170.4
2"	130.7	21.0	116.2	116.9	130.3	20.5
3"	129.7		146.6	146.2	130.1	
4"	128.5		134.2	134.5	128.2	
5"	133.0		128.3	128.4	132.9	
6"	128.5		128.7	128.9	128.2	
7"	129.7		130.5	130.5	130.1	
8"			128.7	128.9		
9"			128.3	128.4		
^a Interchange	eable.					

0 H H 9 7 8 "CH₃" OH 8 "CH₃" OH 8 "CH₃" OH 8 "CH₃" OH 9 CH₃" OCH₃ P R = Bz

Figure 11. Comparison of key ROESY (\leftrightarrow) correlations of 9 and 10.

(7R,8R,2'5,8'R)-Longipedunculata C (3): yellow, amorphous powder; $[\alpha]_D^{20}$ –8 (c 0.2, MeOH); UV (MeOH) $\lambda_{\rm max}$ (log ε) 215 (2.25), 329 (1.18) nm; ECD (c 0.2, MeOH) $[\theta]$ –8.1 × 10³ (223 nm), +6.0 × 10² (254 nm), –5.4 × 10³ (318 nm), +2.3 × 10² (371 nm); IR (KBr) $\nu_{\rm max}$ 3376, 2930, 1728, 1643, 1455, 1307, 1077, 962, 538 cm⁻¹; ¹H and ¹³C NMR data, see Tables 1 and 2; HRESIMS (+) m/z 657.2531 [M + Na]⁺ (calcd for C₃₂H₄₂O₁₃Na, 657.2518).

(aP,7R,8R,8'R)-Longipedunculata D (4): yellow, amorphous powder; $[\alpha]_D^{20}$ –28 (c 0.2, MeOH); UV (MeOH) λ_{\max} (log ε) 218 (2.57), 255 (1.92), 286 (1.54) nm; ECD (c 0.2, MeOH) $[\theta]$ +2.4 × 10^5 (210 nm), -1.3×10^5 (252 nm); IR (KBr) ν_{\max} 3379, 2920, 1581, 1460, 1367, 1081, 973, 535 cm⁻¹; 1 H and 13 C NMR data, see Tables

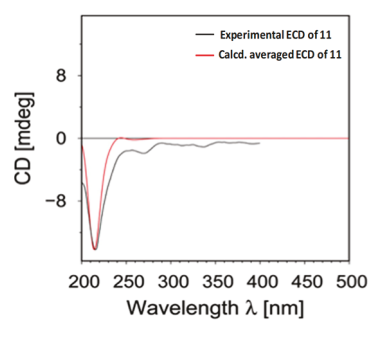


Figure 12. Experimental and calculated averaged Boltzmann-weighted ECD spectra of **11** (red) in MeOH. The σ -value (artificial line broadening) was set to 0.21 eV.

1 and 2; HRESIMS (+) m/z 573.1958 [M + Na]⁺ (calcd for $C_{27}H_{34}O_{12}Na$, 573.1942).

(aM,7 R,8 R,7R)-Longipedlignan K (5): yellow, amorphous powder; $[\alpha]_D^{20}$ +8 (c 0.5, MeOH); UV (MeOH) λ_{\max} ($\log \varepsilon$) 202 (1.40), 220 (1.64) nm; ECD (c 0.5, MeOH) $[\theta]$ -1.3 × 10⁵ (210 nm), +8.5 × 10⁴ (249 nm); IR (KBr) ν_{\max} 3407, 2960, 2936, 2879, 1719, 1650, 1583, 1503, 1488, 1453, 1388, 1262, 1121, 1097, 1064, 1026, 959, 933, 718 cm⁻¹; ¹H and ¹³C NMR data, see Tables 3 and 4; ESIMS (+) m/z 531 [M + Na]⁺; HRESIMS (+) m/z 531.1996 [M + Na]⁺ (calcd for $C_{29}H_{30}O_9Na$, 531.1989).

(7R,8R,2'S,8'R)-Longipedlignan L (6): yellow, amorphous powder; $[\alpha]_D^{20}+13$ (c 0.1, MeOH); ECD (c 0.1, MeOH) $[\theta]-9.5\times10^2$ (214 nm), +1.0 × 10³ (258 nm), -5.8 × 10² (308 nm), +2.6 × 10² (386 nm); IR (KBr) $\nu_{\rm max}$ 3369, 2956, 2926, 2854, 1737, 1678, 1589, 1504, 1490, 1458, 1384, 1249, 1234, 1122, 1100, 1066, 1026, 958, 934 cm⁻¹; ¹H and ¹³C NMR data, see Tables 3 and 4; HRESIMS (+) m/z 449.1210 $[M + Na]^+$ (calcd for $C_{23}H_{22}O_8Na$, 449.1207).

(7R,8S,2'S,8'R)-Longipedlignan M (7): yellow, amorphous powder; $[\alpha]_D^{20}$ – 5.6 (c 0.4, MeOH); UV (MeOH) $\lambda_{\rm max}$ (log ε) 202 (1.64), 219 (1.75), 280 (1.23) nm; ECD (c 0.4, MeOH) [θ] +3.2 × 10³ (212 nm), +4.2 × 10³ (241 nm), -8.2 × 10³ (292 nm), +3.9 × 10³ (371 nm); IR (KBr) $\nu_{\rm max}$ 3578, 3483, 2978, 2838, 1718, 1648, 1578, 1502, 1486, 1450, 1393, 1309, 1261, 1149, 1125, 1089, 1025, 946, 856, 769 cm⁻¹; ¹H and ¹³C NMR data, see Tables 3 and 4; ESIMS (+) m/z 569 [M + Na]*; HRESIMS (+) m/z 569.1792 [M + Na]* (calcd for C₃₁H₃₂O₉Na, 569.1782).

(7R,85,2'5,8'S)-Longipedlignan N (8): yellow, amorphous powder; $[\alpha]_D^{20}-19$ (c 0.1, MeOH); UV (MeOH) $\lambda_{\rm max}$ (log ε) 220 (1.73), 281 (1.22) nm; ECD (c 0.1, MeOH) $[\theta]$ +6.5 × 10 (242 nm), -1.3 × 10² (318 nm), +6.5 × 10 (372 nm); IR (KBr) $\nu_{\rm max}$ 3368, 2955, 2919, 2851, 1717, 1642, 1578, 1543, 1468, 1395, 1311, 1264, 1203, 1158, 1126, 1107, 1065, 1025, 939, 769, 687 cm⁻¹; 1 H and 13 C NMR data, see Tables 3 and 4; ESIMS (+) m/z 569 [M + Na]*; HRESIMS (+) m/z 569.1785 [M + Na]* (calcd for C₃₁H₃₂O₉Na, 569.1782).

(1′S*,2′S,6′S,7′S,8′S,7R,8R)-Longipedlignan O (9): yellow, amorphous powder; $[\alpha]_{\rm D}^{20}$ +20 (c 0.1, MeOH); UV (MeOH) $\lambda_{\rm max}$ (\log ε) 216 (1.76), 268 (1.25) nm; ECD (c 0.1, MeOH) $[\theta]$ –1.2 × 10⁴ (238 nm), +6.6 × 10³ (269 nm); IR (KBr) $\nu_{\rm max}$ 3503, 2985, 2958, 2880, 1717, 1632, 1504, 1454, 1412, 1385, 1316, 1277, 1234, 1110, 1070, 1024, 972, 934, 711 cm⁻¹; 1 H and 13 C NMR data, see Tables 3 and 4; ESIMS (+) m/z 559 [M + Na]*; HRESIMS (+) m/z 559.1581 [M + Na]* (calcd for C_{29} H₂₈O₁₀Na, 559.1575).

(1′S*,2′S,6′S,7′S,8′S,7′R,8R)-Longipedlignan P (10): yellow, amorphous powder; $[\alpha]_{\rm D}^{20}$ +35 (c 0.1, MeOH); UV (MeOH) $\lambda_{\rm max}$ (log ε) 216 (1.74), 263 (1.36) nm; ECD (c 0.1, MeOH) $[\theta]$ –1.1 × 10³ (211 nm), -8.4 × 10² (243 nm), +1.4 × 10³ (272 nm), +0.7 × 10² (361 nm); IR (KBr) $\nu_{\rm max}$ 3359, 2962, 2920, 2852, 1740, 1632, 1505, 1457, 1435, 1381, 1327, 1231, 1111, 1067, 1028, 974, 933 cm⁻¹; ¹H and ¹³C NMR data, see Tables 3 and 4; ESIMS (+) m/z 497 [M + Na]⁺; HRESIMS (+) m/z 497.1436 [M + Na]⁺ (calcd for C₂₄H₂₆O₁₀Na, 497.1418).

(75,8R,8'R)-Longipedlignan Q (11): white, amorphous powder; $[\alpha]_{\rm D}^{20}$ –12 (c 0.2, MeOH); UV (MeOH) $\lambda_{\rm max}$ (log ε) 205 (2.36), 277

(1.29) nm; ECD (c 0.2, MeOH) $[\theta]$ -4.7 × 10⁴ (216 nm); IR (KBr) $\nu_{\rm max}$ 3411, 2963, 2936, 1594, 1510, 1460, 1432, 1348, 1237, 1201, 1140, 1104, 1001, 848, 777 cm⁻¹; ¹H NMR (CDCl₃, 500 MHz) 6.54 (1H, d, J = 2.0 Hz, H-6), 6.51 (1H, d, J = 2.0 Hz, H-2), 6.39 (1H, d, J)= 2.0 Hz, H-2'), 6.38 (1H, d, I = 2.0 Hz, H-6'), 4.35 (1H, d, I = 9.5Hz, H-7), 3.86 (3H, s, -OCH₃), 3.83 (3H, s, -OCH₃), 3.79 (3H, s, $-OCH_3$), 3.78 (3H, s, $-OCH_3$), 2.86 (1H, dd, J = 3.0, 13.0 Hz, H-7'b), 2.38 (1H, m, H-8'), 2.05 (1H, dd, I = 11.0, 13.0 Hz, H-7'a), 1.81 (1H, ddq, J = 3.0, 9.5, 7.5 Hz, H-8), 0.89 (3H, t, J = 7.5 Hz, H-9'), 0.65 (3H, t, J = 7.5 Hz, H-9); ¹³C NMR (CDCl₃, 125 MHz) 139.8 (C-1), 110.9 (C-2), 154.4 (C-3), 142.3 (C-4), 151.3 (C-5), 103.3 (C-6), 77.9 (C-7), 46.3 (C-8), 11.5 (C-9), 136.7 (C-1'), 105.7 (C-2'), 154.2 (C-3'), 135.6 (C-4'), 151.1 (C-5'), 108.9 (C-6'), 38.1 (C-7'), 35.9 (C-8'), 18.5 (C-9'), 61.0 (OCH₃-4, 4'), 56.3 (OCH₃-3, 3'); HRESIMS (+) m/z 429.1893 [M + Na]⁺ (calcd for $C_{22}H_{30}O_7Na_7$) 429.1844).

(7'S,8'R)-Longipedlignan R (12): white, amorphous powder; $[\alpha]_D^{20}$ -7 (c 0.1, MeOH); UV (MeOH) λ_{max} (log ε) 206 (2.18), 268 (1.48) nm; ECD (c 0.1, MeOH) $[\theta]$ +7.8 × 10³ (212 nm), -2.4 × 10⁴ (244 nm); IR (KBr) ν_{max} 3421, 2976, 2937, 2840, 1676, 1594, 1510, 1462, 1425, 1343, 1266, 1228, 1139, 1104, 1058, 1034, 937, 859, 828 cm⁻¹; ¹H NMR (CDCl₃, 500 MHz) 6.96 (1H, d, J = 8.0 Hz, H-5), 6.92 (1H, d, I = 1.5 Hz, H-2), 6.89 (1H, dd, I = 8.0, 1.5 Hz, H-6), 6.57(1H, d, J = 1.5 Hz, H-2'), 6.51 (1H, d, J = 1.5 Hz, H-6'), 6.35 (1H, d)dd, J = 15.5, 1.5 Hz, H-7), 6.16 (1H, dq, J = 15.5, 8.5 Hz, H-8), 4.79 (1H, d, J = 3.0 Hz, H-7'), 4.33 (1H, m, H-8'), 3.90 $(3H, s, OCH_3-4)$, 3.87 (3H, s, OCH₃-3), 3.86 (3H, s, OCH₃-2'), 1.88 (3H, d, J = 6.5Hz, H-9), 1.17 (3H, d, J = 6.5 Hz, H-9'); ¹³C NMR (CDCl₃, 125 MHz) 133.8 (C-1), 109.3 (C-2), 151.8 (C-3), 145.5 (C-4), 120.0 (C-5), 119.0 (C-6), 130.5 (C-7), 125.0 (C-8), 18.4 (C-9), 136.1 (C-1'), 102.0 (C-2'), 152.4 (C-3'), 134.5 (C-4'), 149.0 (C-5'), 105.8 (C-6'), 73.4 (C-7'), 82.3 (C-8'), 13.3 (C-9'), 59.4 (OCH₃-4), 55.7 (OCH₃-3), 60.1 (OCH₃-2'); ESIMS (+) m/z 397 [M + Na]⁺; HRESIMS (+) m/z 397.1635 [M + Na]⁺ (calcd for C₂₁H₂₆O₆Na, 397.1622).

Acid Hydrolysis of 1–4. Authentic sugar samples, D- and L-glucoses (two reactions, 5 mg each), and L-cysteine methyl ester (5 mg) were dissolved in pyridine (1 mL) and heated at 60 °C for 1 h; then o-tolyl isothiocyanate (5 mg) was added to the mixture and heated further for 1 h. The reaction mixture (2 μ L) was analyzed by HPLC and detected at 250 nm. Analytical HPLC was performed on a 250 × 4.6 mm i.d. Cosmosil 5C18-AR II column (Waters, America) at 25 °C with isocratic elution of 25% CH₃CN in 50 mM H₃PO₄ for 25 min at a flow rate of 0.8 mL/min. Peaks were detected with a SPD-M20A photodiode array detector (Shimadzu, Japan).

A solution of each compound (4–6 mg) in 1 N HCl (2.0 mL) was individually refluxed at 80 °C for 6 h. The reaction mixture was extracted with EtOAc (3 × 5 mL), and the aqueous phase was allowed to stand under reduced pressure. The derivation reaction and the analysis process for each residue were repeated similar to those of the authentic sugar samples mentioned above, and the time differences ($\Delta\delta_{\rm D-L}$) were sufficient to distinguish between D- and L-enantiomers. (The detailed results are shown in the Supporting Information.)

Hepatoprotective Activity Assay. All the compounds were tested for hepatoprotective activity against APAP-induced toxicity in HepG2 cells by means of a published MTT method.²⁵ Bicyclol was used as a positive control.

Inhibitory Effects on Nitric Oxide Production Activities Assay. All the compounds were tested for anti-inflammatory activity against lipopolysaccharide (LPS)-induced NO production in macrophages harvested from the peritoneal cells of C57BL/6J male mice by means of a published MTT method. ²⁶ Dexamethasone was used as a positive control. All experiments were done in triplicate.

Molecular Modeling Study. The 2D structures of compounds 1, 4, 5, 6, and 11 were sketched in the 2D-sketcher module in Maestro²⁷ and energy-minimized using the LigPrep²⁸ module implemented in the Schrödinger suite. The conformational sampling of all of the 3D-minimized compounds was carried out with the Macromodel²⁹ program considering 42 kJ/mol as the energy-window cutoff for saving structures. Redundant conformers were eliminated using a root-mean-square deviation cutoff of 0.5 Å. Mixed torsional/low-

mode sampling searches with intermediate torsional sampling were carried out in the gas phase with the maximum number of steps set to 1000. The energy minimization was performed using the Polak-Ribière conjugate gradients method with a convergence threshold of 0.001 kJ/mol. The lowest energy conformers for each compound, those having >1% Boltzmann population, were selected for further geometry optimization.

ECD Calculations. A similar method was used for ECD calculations as previously described.^{6,11} In brief, the conformations that showed >1% Boltzmann population from molecular mechanics calculations were further geometry optimized at the DFT B3LYP/6-31G(d,p) level and subsequently further optimized using the DFT B3LYP/6-311+G(2d,p) level in Gaussian 09 software.³⁰ MeOH was used as a solvent with the polarizable continuum solvent model (PCM).³¹ All the geometry optimizations included subsequent frequency calculations to verify that true minima on the potential energy surface were obtained. The ECD spectra of all the optimized conformers for each compound were calculated using the time-dependent density functional theory³² method with PCM MeOH as the solvent. SpecDis³³ software was used for the generation of the ECD spectral images.

ASSOCIATED CONTENT

S Supporting Information

The Supporting Information is available free of charge on the ACS Publications website at DOI: 10.1021/acs.jnat-prod.9b00576.

¹H NMR, ¹³C NMR, HMBC, HSQC, ¹H-¹H COSY, ROESY, ECD, and HRESIMS data for compounds 1–12, computational details, and the detailed experimental conditions for the hepatoprotective assay (PDF)

AUTHOR INFORMATION

Corresponding Authors

*Tel/Fax (S.L.): +86-10-63164628. E-mail: lishuai@imm.ac.

*Tel/Fax (M.T.H.): +1-843-876-2316. E-mail: hamannm@musc.edu.

ORCID ®

Pankaj Pandey: 0000-0001-9128-8254 Xiaojuan Wang: 0000-0001-5559-6997 Daneel Ferreira: 0000-0002-9375-7920 Robert J. Doerksen: 0000-0002-3789-1842

Shuai Li: 0000-0001-5721-8658

Author Contributions

J.L. and P.P. contributed equally to this work.

Notes

The authors declare no competing financial interest.

ACKNOWLEDGMENTS

This study was supported financially by the CAMS Initiative for Innovative Medicine (CAMS-I2M-1-010). P.P. and R.J.D. were supported in part by grant P20GM104932 from the U.S. National Institutes of Health (NIH) and National Science Foundation (NSF) Major Research Infrastructure Grant #1338056; K.A. was supported by NSF CHE-1460568; their research was conducted in part at the Mississippi Center for Supercomputing Research and in part in a facility constructed with support from research facilities improvement program C06RR14503 from the NIH.

REFERENCES

(1) Angulo, P. N. Engl. J. Med. 2002, 346, 1221-1231.

- (2) Rinella, M. E. JAMA 2015, 313, 2263-2273.
- (3) Nashar, K.; Egan, B. M. Diabetes, Metab. Syndr. Obes.: Targets Ther. 2014, 7, 421-435.
- (4) Pais, R.; Charlotte, F.; Fedchuk, L.; Bedossa, P.; Lebray, P.; Poynard, T.; Ratziu, V.; Group, L. S. J. Hepatol. 2013, 59, 550-556.
- (5) Michaut, A.; Moreau, C.; Robin, M. A.; Fromenty, B. *Liver Int.* **2014**, 34, e171–179.
- (6) Liu, J.; Pandey, P.; Wang, X.; Qi, X.; Chen, J.; Sun, H.; Zhang, P.; Ding, Y.; Ferreira, D.; Doerksen, R. J.; Hamann, M. T.; Li, S. J. Nat. Prod. 2018, 81, 846–857.
- (7) Wang, X.; Liu, J.; Pandey, P.; Fronczek, F. R.; Doerksen, R. J.; Chen, J.; Qi, X.; Zhang, P.; Ferreira, D.; Valeriote, F. A.; Sun, H.; Li, S.; Hamann, M. T. Org. Lett. **2018**, 20, 5559–5563.
- (8) Liu, G. T. Acta Pharm. Sin. B 1987, 8, 560-562.
- (9) Liu, G. T. Prog. Physiol. 1988, 19, 197-203.
- (10) Lu, H.; Liu, G. T. Acta Pharm. Sin. B 1990, 11, 331-335.
- (11) Wang, X.; Liu, J.; Pandey, P.; Chen, J.; Fronczek, F. R.; Parnham, S.; Qi, X.; Doerksen, R. J.; Ferreira, D.; Sun, H. Biochim. Biophys. Acta, Gen. Subj. 2017, 1861, 3089–3095.
- (12) Lu, H.; Liu, G. T. Planta Med. 1992, 58, 311-313.
- (13) Li, L.; Liu, G. T. Acta Pharm. Sin. B 1998, 33, 81-86.
- (14) Chen, D. F.; Zhang, S. X.; Chen, K.; Zhou, B. N.; Wang, P.; Cosentino, L. M.; Lee, K. H. *J. Nat. Prod.* **1996**, *59*, 1066–1068.
- (15) Chen, D. F.; Zhang, S. X.; Xie, L.; Xie, J. X.; Chen, K.; Kashiwada, Y.; Zhou, B. N.; Wang, P.; Cosentino, L. M.; Lee, K. H. *Bioorg. Med. Chem.* **1997**, *5*, 1715–1723.
- (16) Liu, J.; Qi, Y.; Lai, H.; Zhang, J.; Jia, X.; Liu, H.; Zhang, B.; Xiao, P. *Phytomedicine* **2014**, *21*, 1092–1097.
- (17) Pu, J. X.; Yang, L. M.; Xiao, W. L.; Li, R. T.; Lei, C.; Gao, X. M.; Huang, S. X.; Li, S. H.; Zheng, Y. T.; Huang, H.; Sun, H. D. *Phytochemistry* **2008**, *69*, 1266–1272.
- (18) Han, S.; Wang, C.; Cui, B.; Sun, H.; Zhang, J.; Li, S. *Phytochemistry* **2019**, 157, 71–81.
- (19) Yang, J. H.; Zhang, H. Y.; Wen, J.; Du, X.; Chen, J. H.; Zhang, H. B.; Xiao, W. L.; Pu, J. X.; Tang, X. C.; Sun, H. D. *J. Nat. Prod.* **2011**, 74, 1028–1035.
- (20) Shen, Y. C.; Cheng, Y. B.; Lan, T. W.; Liaw, C. C.; Liou, S. S.; Kuo, Y. H.; Khalil, A. T. *J. Nat. Prod.* **2007**, *70*, 1139–1145.
- (21) Chen, D. F.; Zhang, S. X.; Kozuka, M.; Sun, Q. Z.; Feng, J.; Wang, Q.; Mukainaka, T.; Nobukuni, Y.; Tokuda, H.; Nishino, H.; Wang, H. K.; Morris-Natschke, S. L.; Lee, K. H. *J. Nat. Prod.* **2002**, *65*, 1242–1245.
- (22) Sakurai, N.; Nagashima, S. I.; Kawai, K. I.; Inoue, T. Chem. Pharm. Bull. 1989, 37, 3311–3315.
- (23) Gan, M.; Zhang, Y.; Lin, S.; Liu, M.; Song, W.; Zi, J.; Yang, Y.; Fan, X.; Shi, J.; Hu, J.; Sun, J.; Chen, N. J. Nat. Prod. **2008**, 71, 647–654.
- (24) Jaeschke, H.; McGill, M. R.; Williams, C. D.; Ramachandran, A. Life Sci. 2011, 88, 737–745.
- (25) Li, C. J.; Ma, J.; Sun, H.; Zhang, D.; Zhang, D. M. Org. Lett. **2016**, 18, 168–171.
- (26) Liu, J. B.; Ding, Y. S.; Zhang, Y.; Chen, J. B.; Cui, B. S.; Bai, J. Y.; Lin, M. B.; Hou, Q.; Zhang, P. C.; Li, S. J. Nat. Prod. **2015**, 78, 1015–1025.
- (27) Schrödinger Release 2016-1: Maestro; Schrödinger LLC: New York, NY, 2016.
- (28) Schrödinger Release 2016-1: LigPrep; Schrödinger LLC: New York, NY, 2016.
- (29) Schrödinger Release 2016-1: *MacroModel*; Schrödinger LLC: New York, NY, 2016.
- (30) Frisch, M. J.; et al. *Gaussian 09*, revision B.01; Gaussian, Inc.: Wallingford, CT, 2009.
- (31) Mennucci, B.; Tomasi, J. J. Chem. Phys. 1997, 106, 5151-5158.
- (32) Autschbach, J. ChemPhysChem 2011, 12, 3224-3235.
- (33) Bruhn, T.; Schaumlöffel, A.; Hemberger, Y.; Bringmann, G. Chirality 2013, 25, 243–249.